PHYSICAL REVIEW B
CONDENSED MATTER

THIRD SERIES, VOLUME 43, NUMBER 14 15 MAY 1991-I

Coverage dependence of surface optical second-harmonic generation from CO/Ni(110): Investigation with a nonlinear-interference technique

X. D. Zhu
Department of Physics, University of California, Davis, California 95616

Winfried Daum,* Xu-Dong Xiao, R. Chin, and Y. R. Shen
Department of Physics, University of California, Berkeley, California 94720
and Materials Science Division, Lawrence Berkeley Laboratory, Berkeley, California 94720
(Received 31 October 1990)

A nonlinear-optical-interference technique in surface second-harmonic generation is developed to measure directly the variation of surface nonlinear susceptibility of CO/Ni(110) as a function of the CO coverage. It is found that some of the susceptibility elements vary linearly with the coverage and others nonlinearly. A simple model suggests that the former are dominated by contributions from nearly free electrons, while the latter by contributions from the more localized electrons.

I. INTRODUCTION

Optical three-wave mixing, such as second-harmonic generation (SHG) and sum-frequency generation, is being increasingly used in studies of surfaces of metals and semiconductors.[1-5] Atomic or molecular adsorption to such surfaces is of great interest to many researchers. The surface nonlinear optical response can provide useful information about surface properties of a medium and how they are affected by adsorption. In addition, it can be used as an *in situ* probe to study surface dynamics of adsorbates such as adsorption, desorption, and surface diffusion.[1-6] However, it is known that even though three-wave mixing is forbidden, under the electric-dipole approximation, in a medium with inversion symmetry, the bulk can still contribute via electric quadrupole and other multipole radiation to the signal reflected from a surface.[7] The surface nonlinearity itself contains two parts: one adsorption-free and the other adsorption-related. In order to deduce the adsorption-related part of the surface nonlinearity from measurements and use it to study adsorbates on a surface, care must be taken to properly subtract the adsorption-free part (including the bulk contribution). This is nontrivial because, in general, surface nonlinear optical susceptibilities are complex quantities. Different contributions can lead to terms in a nonlinear susceptibility with different phases, and there is no prior knowledge of these phases.

In the literature, many authors have adopted simplifying assumptions for the effective surface nonlinear susceptibilities (including the bulk contribution) to interpret their surface SHG results.[8-12] In all cases, they assumed that the relative phase of the adsorption-related part with respect to the adsorption-free part in the susceptibility is constant, independent of the coverage of the adsorbates. Then with a limited number of variables as fitting parameters, the adsorption-related part as a function of the coverage of adsorbates can be deduced. This turns out to be reasonable in some cases, but yields wrong results in other cases.

Ideally, one may want to deduce the adsorption-related term of the surface nonlinear susceptibility directly from measurements. This is actually possible with an interference method.[13] The adsorption-free contribution to the SH signal can, in principle, be exactly canceled by a contribution with the opposite sign from a properly adjusted nonlinear medium inserted in the beam path. The observed SH signal then solely comes from the adsorption-related contribution. In this paper, we report the development of such a technique to study CO adsorption on Ni(110). We have measured four of the five independent surface susceptibility elements as functions of the CO coverage using both the polarization dependence and the interference technique. We found that the susceptibility elements generally do not vary linearly with the coverage. The change of local density of states near the Fermi level at the surface and the CO-CO interaction upon CO adsorption are presumably responsible for the observation. Our paper is organized as follows: In Sec. II we discuss explicitly the surface nonlinear susceptibilities and the interference method employed to suppress the adsorption-free part. Section III briefly describes the sample

preparation and experimental arrangement. Finally, in Secs. IV and V, respectively, experimental results are presented and discussed.

II. SURFACE NONLINEAR SUSCEPTIBILITIES

We consider here SHG in reflection from a metal surface. As shown elsewhere, the SH signal S is directly proportional to the absolute square of an effective surface nonlinear susceptibility $\chi^{(2)}_{\rm eff}$,[1]

$$S_i \propto |\chi^{(2)}_{{\rm eff},ijk}|^2 , \tag{1}$$

where the subscripts i,j,k denote the polarizations of the SH output and the two fundamental inputs, respectively. Since the proportional constant of the relation in Eq. (1) is known, measurement of S_i allows us to deduce $|\chi^{(2)}_{{\rm eff},ijk}|$. Generally, $\chi^{(2)}_{{\rm eff},ijk}$ consists of a bulk term and a surface term; the latter can be further decomposed into an adsorption-free part and an adsorption-related part. We can thus write

$$\begin{aligned}\chi^{(2)}_{\rm eff}(\theta) &= \chi^{(2)}_s(\theta) + B\chi^{(2)}_{\rm bulk} \\ &= \Delta\chi^{(2)}(\theta) + \chi^{(2)}_s(0) + B\chi^{(2)}_{\rm bulk} .\end{aligned} \tag{2}$$

Here, $\chi^{(2)}_s$ and $\chi^{(2)}_{\rm bulk}$ refer to surface and bulk nonlinear susceptibilities, respectively, B is a known constant depending on the experimental geometry, θ denotes the coverage of adsorbates, and $\Delta\chi^{(2)}(\theta) \equiv \chi^{(2)}_s(\theta) - \chi^{(2)}_s(0)$ is the adsorption-related part of $\chi^{(2)}_s$ that vanishes when $\theta = 0$.

For adsorption studies, we are normally interested in $\Delta\chi^{(2)}_s(\theta)$. It is possible, in principle, to deduce $\Delta\chi^{(2)}(\theta)$ by measuring the complex quantities of $\chi^{(2)}_{\rm eff}(\theta)$ at various θ. However, this would be rather tedious and inaccurate. A better way is to obtain $\Delta\chi^{(2)}(\theta)$ directly from measurements. This can be achieved by suppressing $\chi^{(2)}_s(0) + B\chi^{(2)}_{\rm bulk}$ in SHG measurements using an interference technique.[13,14]

Consider the insertion of a nonlinear crystal (e.g., a thin crystalline quartz plate) in the beam path after reflection from the sample. The SH signal reaching the detector is now given by

$$S' \propto |\Delta E(\theta) + E_s(0) + E_Q|^2 , \tag{3}$$

with

$$\Delta E(\theta) \propto \Delta\chi^{(2)}(\theta) ,$$

$$E_s(0) \propto \chi^{(2)}_s(0) + B\chi^{(2)}_{\rm bulk} ,$$

$$E_Q = |E_Q| \exp(i\phi) ,$$

where E_Q is from the inserted nonlinear crystal. The amplitude $|E_Q|$ can be adjusted by varying the orientation of the nonlinear crystal and the phase ϕ by varying the optical path length between the crystal and the sample. If we let $E_Q = -E_s(0)$, then we have

$$S' \propto |\Delta E(\theta)|^2 \propto |\Delta\chi^{(2)}(\theta)|^2 , \tag{4}$$

from which we can deduce $\Delta\chi^{(2)}(\theta)$ directly.

A Ni(110) surface has C_{2v}, or $mm2$, point-group symmetry. Accordingly, there are five independent surface nonlinear susceptibility elements,[15]

$$\chi^{(2)}_{xzx},\ \chi^{(2)}_{yzy},\ \chi^{(2)}_{zxx},\ \chi^{(2)}_{zyy},\ \chi^{(2)}_{zzz} .$$

The $\hat{\mathbf{x}}$ and $\hat{\mathbf{y}}$ axes refer to the $[1\bar{1}0]$ and [001] directions in the surface plane, respectively, and $\hat{\mathbf{z}}$ coincides with the surface normal. These susceptibility elements can be deduced separately from SHG measurements using different input-output polarization combinations. With the $\hat{\mathbf{x}}$ axis in the plane of incidence, s-polarized fundamental inputs and a p-polarized SH output (s-in, p-out geometry) yield $\chi^{(2)}_{zyy}$; inputs with mixed s and p polarizations and a SH output with s polarization (mixed-in, s-out) give $\chi^{(2)}_{yzy}$. Similarly, with the $\hat{\mathbf{y}}$ axis in the plane of incidence, the s-in, p-out and mixed-in, s-out geometries measure $\chi^{(2)}_{zxx}$ and $\chi^{(2)}_{xzx}$, respectively. Finally, with the $\hat{\mathbf{x}}$ axis in the plane of incidence, the p-in, p-out geometry yields $\chi^{(2)}_{xzx} + a\chi^{(2)}_{zxx} + b\chi^{(2)}_{zzz}$ from which $\chi^{(2)}_{zzz}$ can be deduced knowing $\chi^{(2)}_{xzx}$ and $\chi^{(2)}_{zxx}$. The coefficients a and b are constants determined by Fresnel factors. As an independent check, one can arrange to have the plane of incidence bisect the $\hat{\mathbf{x}}$ and $\hat{\mathbf{y}}$ axes. Then, a p-in, s-out geometry gives $\chi^{(2)}_{yzy} - \chi^{(2)}_{xzx}$.

III. SAMPLE PREPARATION AND EXPERIMENTAL APPARATUS

The experiment was performed with a Ni(110) sample mounted in an ultra-high-vacuum chamber with an operating pressure of 1×10^{-10} Torr. A clean surface of Ni(110) was obtained by one cycle of Ar^+ sputtering (1.0×10^{-4} Torr, 500 eV ion energy) at room temperature for 30 min and subsequent annealing at 1070 K for a few seconds before slowly cooling down to the measurement temperature. Auger electron spectra of the clean Ni(110) surface revealed no traces of contamination within the detection limit ($<0.5\%$ for sulfur, and $<0.3\%$ for carbon). CO was dosed to the sample through a variable leak value and the dosage was monitored by a partial-pressure measurement. To convert dosage to coverage, we used the calibration obtained from the work-function measurement and the thermal-desorption measurement by Behm, Ertl, and Penka.[16] The sample temperature was kept at 100 K during CO dosing and the optical SHG measurement.

The experimental arrangement is shown in Fig. 1(a). For the probe beam, we used laser pulses at 0.532 μm obtained by frequency-doubling the output of a 10-ns Q-switched Nd:YAG (yttrium aluminum garnet) laser. It was incident on the sample at either 45° or 70° relative to the surface normal. The second-harmonic signal in reflection was detected with a photomultiplier tube and a gated electronic system. The polarizations of the probe beam and the SH beam were independently set and analyzed so that different surface susceptibility elements could be measured separately.

Our sample manipulator was capable of rotating the sample about its surface normal. This facilitates the measurement of different second-harmonic susceptibility elements defined in the crystal coordinate system with the

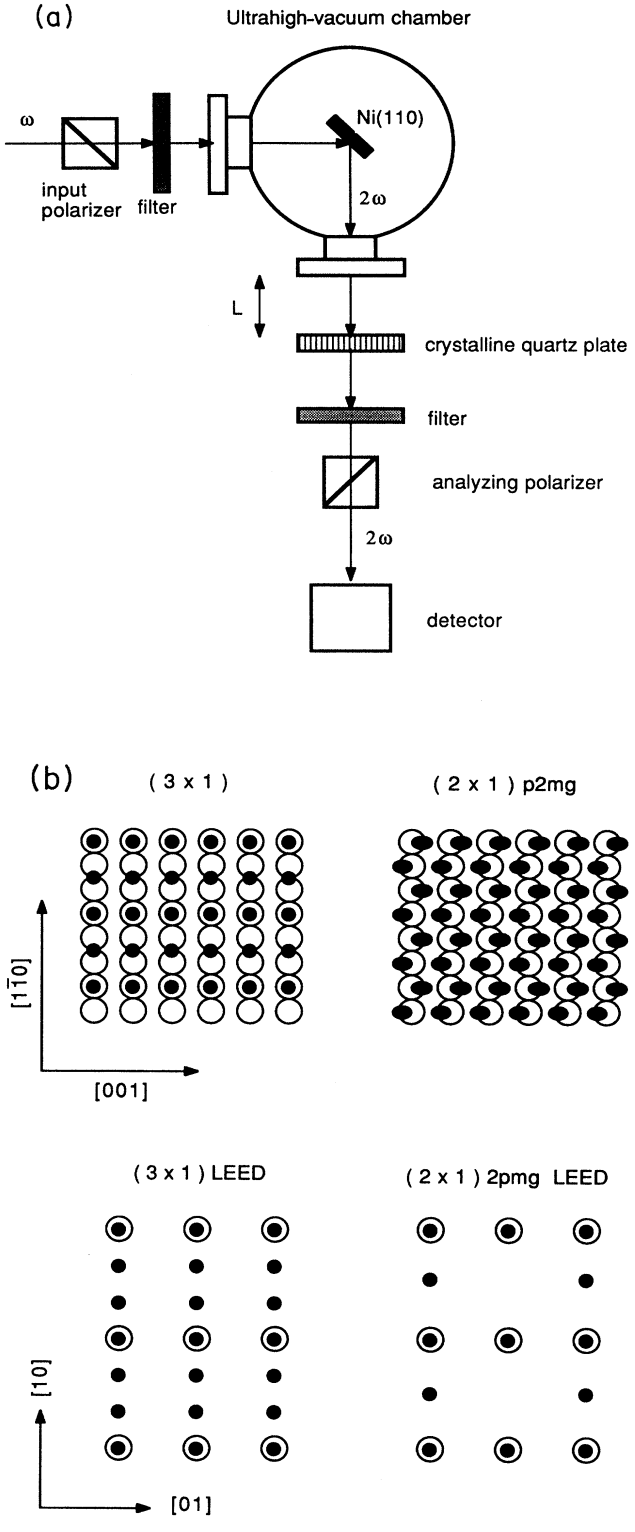

FIG. 1. (a) Schematic of the experimental setup. (b) Low-energy electron-diffraction (LEED) patterns and the corresponding real-space superstructure of CO on Ni. The open circles denote the Ni(110) atoms, and the solid circles the CO molecules.

[1$\bar{1}$0] crystallographic direction along the $\hat{\mathbf{x}}$ axis. The SHG measurements were performed at three azimuthal orientations of the sample: [1$\bar{1}$0] in the plane of incidence, [001] in the plane of incidence, and [1$\bar{1}$0] and [001] both at 45° from the plane of incidence. At each orientation, the SH signals were measured with appropriate input-output polarization combinations.

For the measurements with the interference technique, a thin crystalline quartz plate was placed outside the UHV chamber before the filter as shown in Fig. 1(a). The crystallographic $\hat{\mathbf{x}}$ and $\hat{\mathbf{z}}$ axes of the quartz plate lay in the surface plane. With the input laser beam normally incident on the plate, the SH output was along the quartz $\hat{\mathbf{x}}$ axis. If the input is polarized at an angle ψ from the $\hat{\mathbf{x}}$ axis, then the SH output is proportional to $\cos^2\psi$. Since the fundamental and SH beams travel in air with different phase velocities

$$n(\lambda=0.266\mu\text{m})-n(\lambda=0.532\mu\text{m})=2.0\times10^{-5}\ ,$$

the relative phase of the SH field generated from the quartz plate depends on the beam path L as shown in Fig. 1. Thus by varying ψ and L in our experiment, we could vary $|E_Q|$ and ϕ to cancel $E_s(0)$ in Eq. (3). After nulling the signal from the clean Ni(110) surface, the measured SHG signal with the adsorption of CO was directly related to $\Delta\chi^{(2)}(\theta)$ as described in Eq. (4). Knowing $|\chi^{(2)}_{\text{eff}}(0)|$, $|\chi^{(2)}_{\text{eff}}(\theta)|$, and $|\Delta\chi^{(2)}(\theta)|$, we can also deduce, from Eq. (2), the relative phase of $\Delta\chi^{(2)}(\theta)$ as a function of θ.

IV. EXPERIMENTAL RESULTS

A. Adsorption of CO on Ni(110) at 100 K: Low-energy electron-diffraction study

The adsorption of CO on Ni(110) around 100 K has been extensively studied with a number of techniques by other groups.[16–25] The results are summarized as follows. Low-energy electron-diffraction (LEED) studies revealed different adsorption configurations, depending upon the CO coverage.[16,17] At coverage θ above 0.85 of a full monolayer, a (2×1) superstructure with $p2mg$ glide-mirror symmetry has been consistently observed.[16,20,22] For $0.5<\theta<0.85$, intermediate $c(8\times2)$ and $c(4\times2)$ structures were reported.[16,17] Two CO stretch vibrations with frequencies of 1880–1910 and 2020–2040 cm^{-1} were identified by high-resolution electron-energy-loss spectroscopy (HREELS) for coverages between 0.2 and 0.75, corresponding to short-bridge and on-top sites.[22,25] The integrated intensity ratio $I_{\text{top}}/I_{\text{bridge}}$ of these two vibration bands was about 1.2, and practically independent of the coverage.[25] For $\theta>0.75$, the adsorbed CO molecules are compressed towards the on-top sites and tilted away from the surface normal by about 20° to leave space for additional molecules.[23,25] The results of our LEED measurements were partly at variance with those reported in Ref. 16. We did not observe any superstructure at CO coverage below $\theta=0.6$. Between $\theta=0.6$ and 0.7, we consistently observed a sharp (3×1) pattern, which has never been reported before. We propose that it corresponds to a real-

space superstructure with CO alternately occupying on-top and short-bridge sites along the [1$\bar{1}$0] direction, with equal populations on both sites (see Fig. 1). This observation and our assignment agree with the conclusions of the above-cited HREELS measurement if one assumes roughly equal strengths for the CO stretch vibrations on both sites (we have not been able to find an explanation why our LEED observation is different from those of Ref. 16 for intermediate coverages). As the coverage was increased from $\theta=0.7$ to 1, we observed a coexistent phase with the (3×1) structure slowly fading away and the (2×1) $p2mg$ superstructure becoming bright and sharp. From these results, we expect that the nonlinear optical response of the surface has a relatively simple dependence on the CO coverage at $\theta<0.6$.

B. SHG from CO/Ni(110) with *p*-in, *p*-out geometry along [1$\bar{1}$0]

We consider first SHG from Ni(110) in the *p*-in, *p*-out geometry. This is the geometry often used by others as it usually gives the strongest signal from a metal surface. We show in Fig. 2(a) the SH signal as a function of the CO coverage obtained with the plane of incidence along [1$\bar{1}$0]. The incident angle was 70° (45° in all the other cases described later). It is seen that the SH signal decreases by 45% from $\theta=0$ to 0.65 and then recovers at $\theta=1-80\,\%$ of the signal level from the clean surface. Such a nonmonotonic behavior of optical SHG has been observed by others on other adsorbate-covered metal surfaces.[10,26,27] The surface-resonance-shift model and the nearly-free-electron model with electron transfer between the metal substrate and the adsorbate layer have been suggested to explain the observation. However, the nonmonotonic behavior could be caused entirely by interference between the adsorption-free part and the adsorption-related part of the nonlinear response, i.e., between $\chi^{(2)}_{\rm eff}(0)$ and $\Delta\chi^{(2)}(\theta)$. For example, the observation can be qualitatively interpreted if we take $\chi^{(2)}_{\rm eff}(0)$ as real and assume that $\Delta\chi^{(2)}_s(\theta)$ is complex, and has a real part varying monotonically with CO coverage and opposite in sign but larger in magnitude than $\chi^{(2)}_{\rm eff}(0)$ at $\theta=1$. If this is the case, we should expect a monotonic increase of the SH signal, provided that $\chi^{(2)}_{\rm eff}(0)$ is suppressed. As discussed earlier, this can be achieved by the interference technique. With the suppression of $\chi^{(2)}_{\rm eff}(0)$, the SH signal is proportional to $|\Delta\chi^{2}(\theta)|^2$. The results of such measurements on CO/Ni(110) are also presented in Fig. 2(a). For $0<\theta<0.4$, the SH signal (or $|\Delta\chi^{(2)}(\theta)|^2$) increases linearly; for $0.4<\theta<1$, it varies also almost linearly but with a noticeably smaller slope. Consequently, unlike in many cases reported in the literature, $\Delta\chi^{(2)}(\theta)$ does not change linearly with the coverage for CO/Ni(110). In Fig. 2(b), we plot the cosine of the phase of $\Delta\chi^{(2)}(\theta)/\chi^{(2)}_{\rm eff}(0)$, calculated from the two curves in Fig. 2(a). It decreases monotonically from 0 to -0.8 as θ changes from 0 to 1. The results here demonstrate the usefulness and effectiveness of the interference technique. For the *p*-in, *p*-out geometry, however, three surface susceptibility elements contribute to the SH signal as discussed in Sec. II. In order to separately determine each of them, we need to use other polarization combinations.

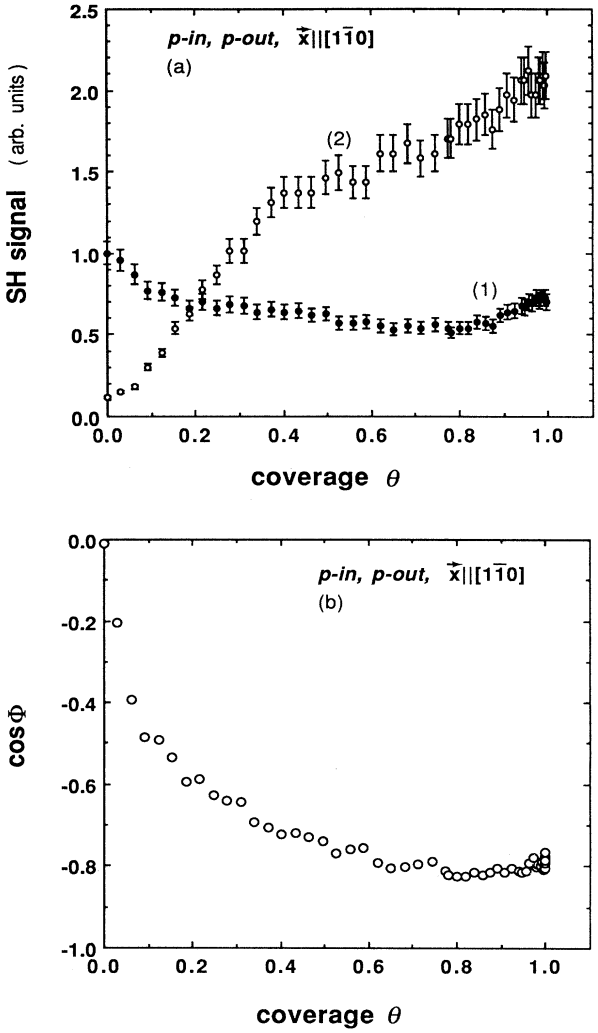

FIG. 2. (a) SH signals vs CO coverage in the *p*-in, *p*-out geometry with [1$\bar{1}$0] in the plane of incidence. Curve (1): $S\sim|\chi^{(2)}_{\rm eff}(0)+\Delta\chi^{(2)}_s(\theta)|^2$. Curve (2): $S\sim|\Delta\chi^{(2)}_s(\theta)|^2$. (b) Cosine of the phase angle Φ of $\Delta\chi^{(2)}_s(\theta)/\chi^{(2)}_{\rm eff}(0)$ vs CO coverage for SHG in the *p*-in, *p*-out geometry.

C. SHG from CO/Ni(110) with *s*-in, *p*-out geometry along [001]

SHG with the *s*-in, *p*-out geometry and the plane of incidence along [001] yields the surface susceptibility element $\chi^{(2)}_{zxx}$. Figure 3(a) shows the results of $|\Delta\chi^{(2)}_{zxx}(\theta)|^2$ and $|\chi^{(2)}_{{\rm eff},zxx}(\theta)|^2$ obtained with and without the use of the interference technique. In both cases, the signal increases almost linearly with θ. This indicates that $|\Delta\chi^{(2)}_{zxx}(\theta)|$ is proportional to $\sim\theta^{1/2}$. In our experiment, due to the inherent optical inhomogeneity of the exit window, the wave fronts of the reflected fundamental and SH beams from the sample were distorted. A complete destructive

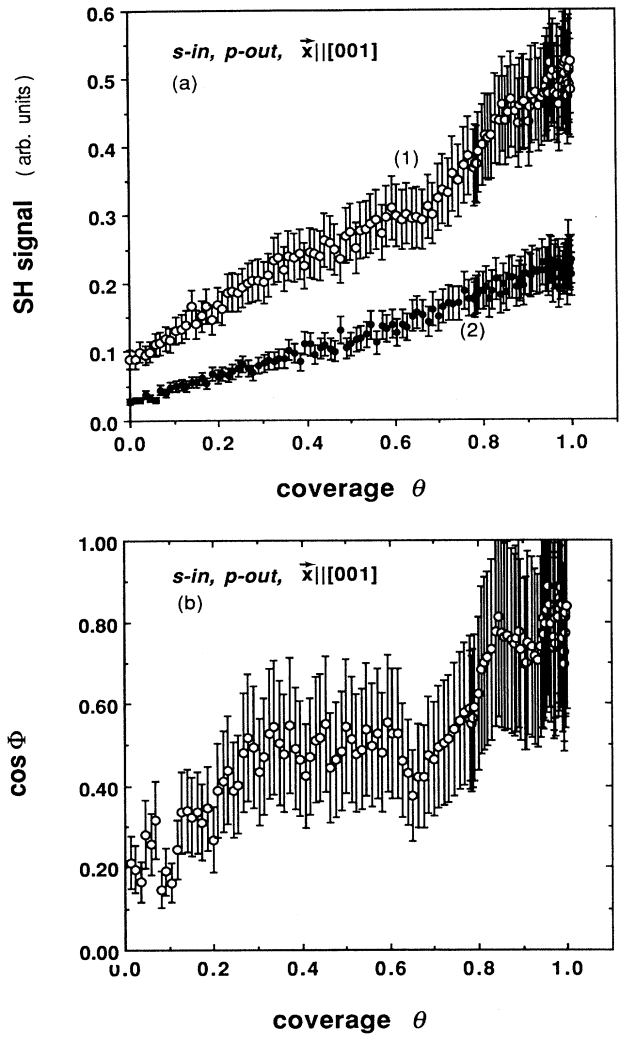

FIG. 3. (a) SH signal vs CO coverage in the s-in, s-out geometry with [001] in the plane of incidence. Curve (1): $S \sim |\chi^{(2)}_{\text{eff},zxx}(0)+\Delta\chi^{(2)}_{zxx}(\theta)|^2$. Curve (2): $S \sim |\Delta\chi^{(2)}_{zxx}(\theta)|^2$. (b) Cosine of the phase angle Φ of $\Delta\chi^{(2)}_{zxx}(\theta)/\chi^{(2)}_{\text{eff},zxx}(0)$ vs CO coverage.

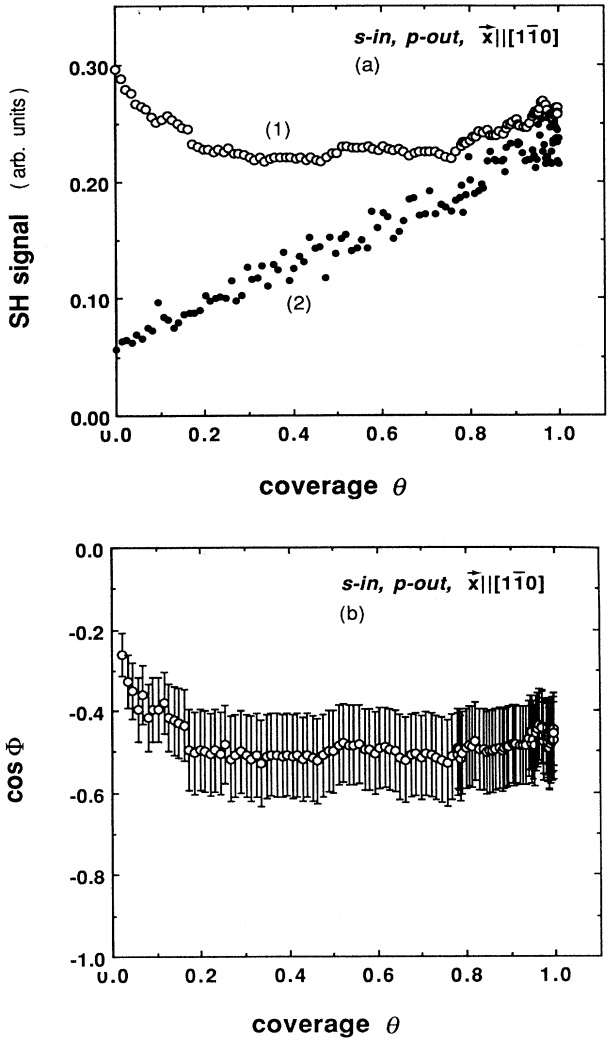

FIG. 4. (a) SH signal vs CO coverage in the s-in, p-out geometry with [1$\bar{1}$0] in the plane of incidence. Curve (1): $S \sim |\chi^{(2)}_{\text{eff},zyy}(0)+\Delta\chi^{(2)}_{zyy}(\theta)|^2$. Curve (2): $S \sim |\Delta\chi^{(2)}_{zxx}(\theta)|^2$. (b) Cosine of the phase angle Φ of $\Delta\chi^{(2)}_{zyy}(\theta)/\chi^{(2)}_{\text{eff},zyy}(0)$ vs CO coverage.

interference across the beam was not possible. This results in a nonzero minimum SH signal even with the optimum adjustment of interference. In the analysis, we assumed that the phase variation over the cross section of the SH signal beam was random. The increase of the SH signal should then be proportional to $|\Delta\chi^{(2)}_{zxx}(\theta)|^2$. The cosine of the phase of $\Delta\chi^{(2)}_{zxx}(\theta)/\chi^{(2)}_{\text{eff},zxx}(0)$ calculated from $|\Delta\chi^{(2)}_{zxx}(\theta)|$ and $|\chi^{(2)}_{\text{eff},zxx}(\theta)|$ is plotted in Fig. 3(b) as a function of θ. It increases with the coverage from 0.2 to 0.8.

D. SHG from CO/Ni(110) with s-in, p-out geometry along [1$\bar{1}$0]

SHG with the s-in, p-out geometry and the [1$\bar{1}$0] direction in the plane of incidence measures the element $\chi^{(2)}_{zyy}$. The results are shown in Figs. 4(a) and 4(b). It is seen that $|\chi^{(2)}_{\text{eff},zyy}(\theta)|^2$ and $|\Delta\chi^{(2)}_{zyy}(\theta)|^2$ behave very differently. While $|\chi^{(2)}_{\text{eff},zyy}(\theta)|^2$ exhibits a shallow minimum, $|\Delta\chi^{(2)}_{zyy}(\theta)|^2$ increases monotically (almost linearly) with θ. Thus $|\Delta\chi^{(2)}_{zyy}(\theta)| \propto \theta^{1/2}$. The cosine of the phase of $\Delta\chi^{(2)}_{zyy}(\theta)/\chi^{(2)}_{\text{eff},zyy}(0)$ is not a constant either, but decreases from -0.25 to -0.5 as θ changes from 0 to 1.

E. SHG from CO/Ni(110) with mixed-in, s-out geometry along [1$\bar{1}$0]

SHG with the mixed-in, s-out geometry and the [1$\bar{1}$0] direction in the plane of incidence gives $\chi^{(2)}_{yzy}$. We did not use the interference technique in this case because the mixed input polarizations complicated the situation and made the cancellation of the adsorption-free part difficult in our setup. As shown in Fig. 5, however, the SH signal

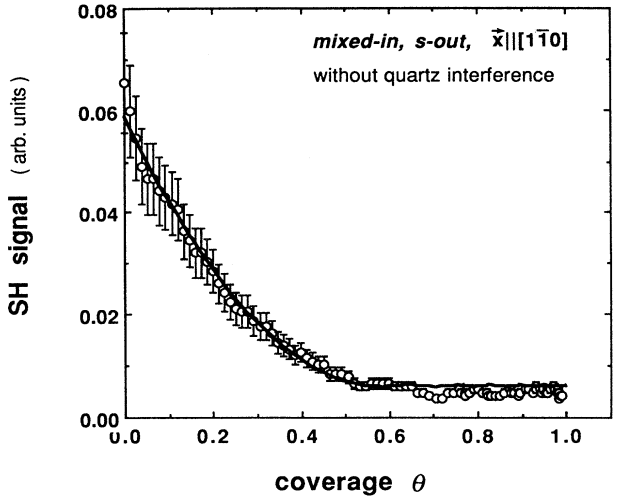

FIG. 5. SH signal, $S \sim |\chi^{(2)}_{yzy}(\theta)|^2$ vs CO coverage in the mixed in, s-out geometry with [001] in the plane of incidence. The solid line is a fit to the experimental data using a linear function of θ for $\Delta\chi^{(2)}_{yzy}(\theta)$.

proportional to $|\chi^{(2)}_{\text{eff},yzy}(\theta)|^2$ can be well fitted with

$$\chi^{(2)}_{\text{eff},yzy}(\theta)=\begin{cases}0.24+0.4e^{i160^\circ}\theta, & 0\le\theta\le 0.60\\ 0.24+0.24e^{i160^\circ}\theta, & 0.60\le\theta\le 1\end{cases}. \quad (5)$$

Note that $\theta\sim 0.65$ is the CO coverage at which a (3×1) superstructure was observed in our experiment. Here, we find that $\Delta\chi^{(2)}_{yzy}(\theta)\propto\theta$ for $\theta<0.60$ and the relative phase between $\Delta\chi^{(2)}_{yzy}(\theta)$ and $\chi^{(2)}_{\text{eff},yzy}(0)$ is constant for all θ.

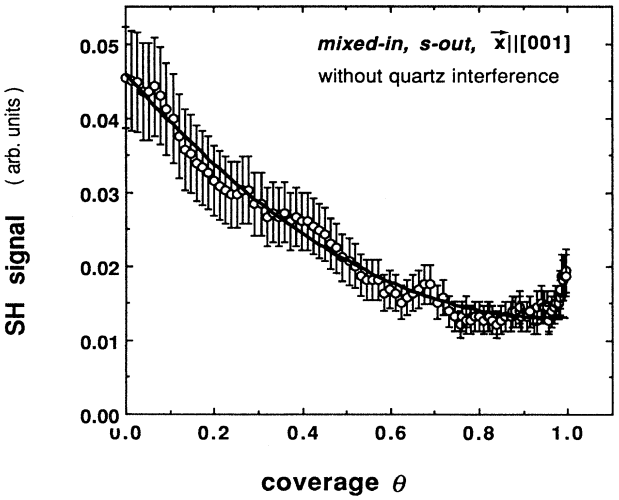

FIG. 6. SH signal, $S \sim |\chi^{(2)}_{\text{eff},xzx}(0)+\Delta\chi^{(2)}_{xzx}(\theta)|^2$ vs CO coverage in the mixed-in, s-out geometry with [001] in the plane of incidence. The solid line is a fit to the experimental data using a linear function of θ for $\Delta\chi^{(2)}_{xzx}(\theta)$.

F. SHG from CO/Ni(110) with mixed-in, s-out geometry along [001]

SHG with the mixed-in, s-out geometry and the plane of incidence along [001] measures $\chi^{(2)}_{xzx}$. Again, we did not apply the interference technique to this case. The data on $|\chi^{(2)}_{\text{eff},xyx}(\theta)|^2$ can again be fitted with the simple expression

$$\chi^{(2)}_{\text{eff},xzx}(\theta)=0.21+0.19e^{i150^\circ}\theta\ , \quad (6)$$

except for $\theta\gtrsim 0.95$, as shown in Fig. 6. Here, we also find $\Delta\chi^{(2)}_{xzx}(\theta)\propto\theta$, and with a constant phase factor with respect to $\chi^{(2)}_{\text{eff},xzx}(0)$.

G. SHG from CO/Ni(110) with p-in, s-out geometry and the plane of incidence bisecting [1$\bar{1}$0] and [001]

This geometry allows an independent check of the results $\Delta\chi^{(2)}_{xzx}(\theta)\propto\theta$ and $\Delta\chi^{(2)}_{yzy}(\theta)\propto\theta$. As mentioned earlier in Sec. II, the measurement gives $\chi^{(2)}_{yzy}(\theta)-\chi^{(2)}_{xzx}(\theta)$. The data are presented in Figs. 7(a)–7(c). We find that the results on $|\chi^{(2)}_{\text{eff},yzy}(\theta)-\chi^{(2)}_{\text{eff},xzx}(\theta)|^2$ in Fig. 7(b) can be fitted very well with Eqs. (5) and (6) as expected. The data on $|\Delta\chi^{(2)}_{yzy}(\theta)-\Delta\chi^{(2)}_{xzx}(\theta)|^2$ in Fig. 7(a) obtained with the interference technique, can also be fitted with use of the θ-dependent terms in Eqs. (5) and (6), although the results at smaller θ might be more affected by the imperfection of the interference technique. The cosine of the relative phase between $[\Delta\chi^{(2)}_{yzy}(\theta)-\Delta\chi^{(2)}_{xzx}(\theta)]$ and $[\chi^{(2)}_{\text{eff},yzy}(0)-\chi^{(2)}_{\text{eff},xzx}(0)]$ shown in Fig. 7(c) indeed appears constant.

H. Deduction of $\Delta\chi^{(2)}_{zzz}(\theta)$

As we mentioned earlier, the p-in, p-out geometry yields an effective susceptibility

$$\Delta\chi^{(2)}_{\text{eff}}(\theta)=\Delta\chi^{(2)}_{xzx}(\theta)+a\,\Delta\chi^{(2)}_{zxx}(\theta)+b\,\Delta\chi^{(2)}_{zzz}(\theta)\ ,$$

with the coefficients a and b determined by the Fresnel factors. Then knowing $\Delta\chi^{(2)}_{xzx}(\theta)$ and $\Delta\chi^{(2)}_{zxx}(\theta)$ from other measurements, we could deduce $\Delta\chi^{(2)}_{zzz}(\theta)$. Unfortunately, we were not able to do so in our experiment because of difficulties in the calibration of signals measured in different geometries.

However, we can extract some information on the relative magnitude of $\Delta\chi^{(2)}_{zzz}(\theta=1)$ in comparison with $\Delta\chi^{(2)}_{xzx}(\theta=1)$ and $\Delta\chi^{(2)}_{zxx}(\theta=1)$. We can explicitly evaluate the coefficients, a and b using material constants for a Ni single crystal,

$$n(\lambda=0.532\ \mu\text{m})=1.75+i3.19\ ,$$
$$n(\lambda=0.266\ \mu\text{m})=1.59+i2.1\ ,$$

in Ref. 28. For incidence angles $\phi_{\text{in}}=45^\circ$ and 70°, we ob-

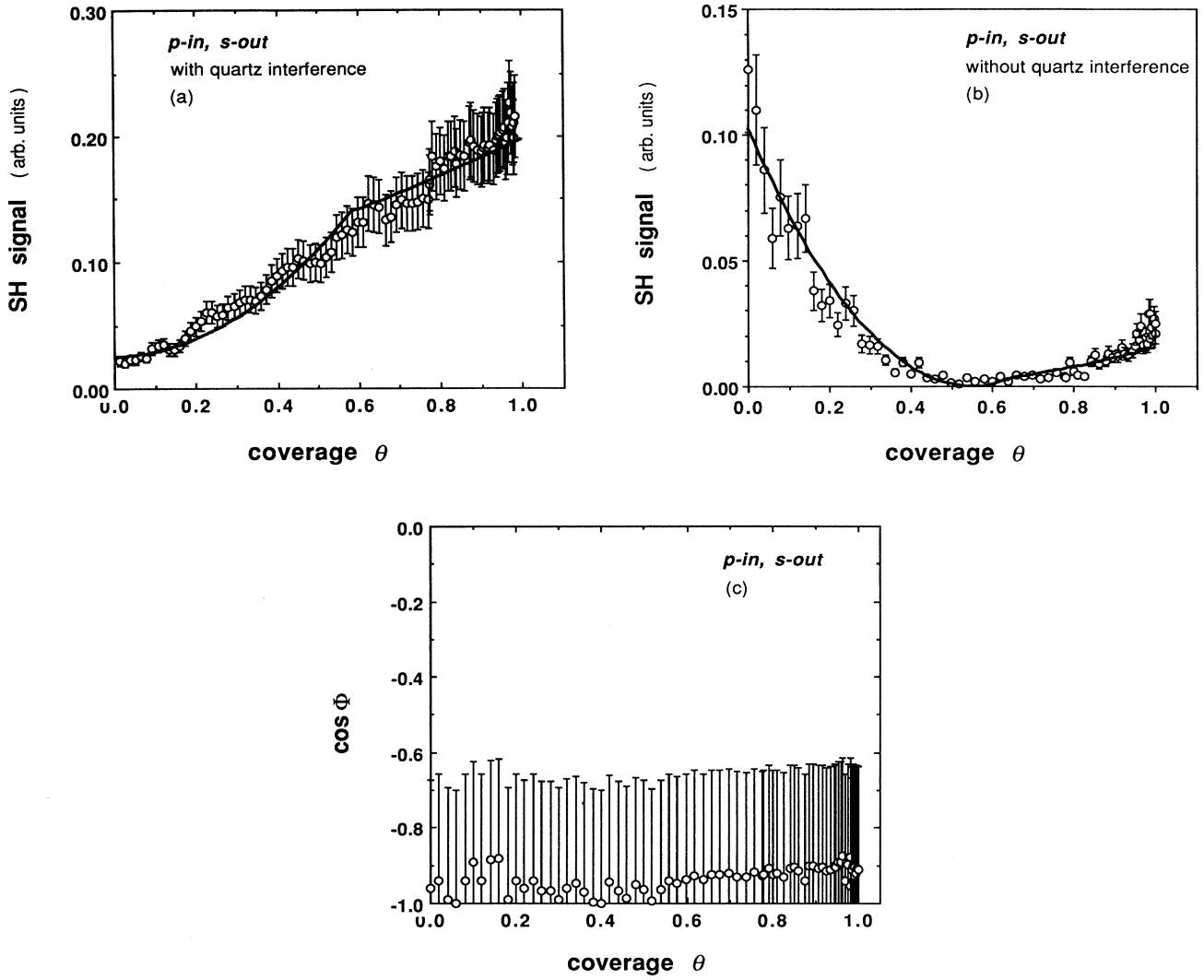

FIG. 7. (a) SH signal, $S \sim |\chi^{(2)}_{\text{eff},yzy}(0)+\Delta\chi^{(2)}_{yzy}(\theta)-\chi^{(2)}_{\text{eff},xzx}(0)-\Delta\chi^{(2)}_{xzx}(\theta)|^2$ vs CO coverage in the p-in, s-out geometry with $[1\bar{1}0]$ and [001] at 45° from the plane of incidence. The solid line is calculated using the parameters in Eqs. (5) and (6). (b) SH signal, $S \sim |\Delta\chi^{(2)}_{yzy}(\theta)-\Delta\chi^{(2)}_{xzx}(\theta)|^2$, vs CO coverage in the same geometry as in (a). The solid line is calculated using the parameters in Eqs. (5) and (6). (c) Cosine of the phase angle Φ of $[\Delta\chi^{(2)}_{yzy}(\theta)-\Delta\chi^{(2)}_{xzx}(\theta)]/[\chi^{(2)}_{\text{eff},yzy}(0)-\chi^{(2)}_{\text{eff},xzx}(0)]$, vs CO coverage.

tain, respectively

$$[\chi^{(2)}_{\text{eff}}(\theta)]_{45°} = \Delta\chi^{(2)}_{xzx}(\theta)+0.68e^{i180°}\Delta\chi^{(2)}_{zxx}(\theta) +0.021e^{i63.6°}\Delta\chi^{(2)}_{zzz}(\theta)$$

and

$$[\Delta\chi^{(2)}_{\text{eff}}(\theta)]_{70°}=\Delta\chi^{(2)}_{xzx}(\theta)+0.68e^{i180°}\Delta\chi^{(2)}_{zxx}(\theta) +0.044e^{i61.3°}\Delta\chi^{(2)}_{zzz}(\theta)\ .$$

Our measurements gave

$$|\Delta\chi^{(2)}_{\text{eff}}(\theta=1)|_{70°}\simeq 1.3|\Delta\chi^{(2)}_{\text{eff}}(\theta=1)|_{45°}\ .$$

This suggests that $|\Delta\chi^{(2)}_{zzz}(\theta=1)|$ is at least 20–50 times larger than $|\Delta\chi^{(2)}_{xzx}(\theta=1)|$ and $|\Delta\chi^{(2)}_{zxx}(\theta=1)|$, although its contribution to $\Delta\chi^{(2)}_{\text{eff}}(\theta)$ is comparable to those of $\Delta\chi^{(2)}_{zxx}(\theta)$ and $\Delta\chi^{(2)}_{xzx}(\theta)$.

I. Summary of experimental results

In summary of the experimental results described above, we find the following.

(i) Both $\Delta\chi^{(2)}_{zyy}(\theta)$ and $\Delta\chi^{(2)}_{zxx}(\theta)$ vary approximately as $\theta^{1/2}$. Their phases change with θ nonlinearly.

(ii) $\Delta\chi^{(2)}_{xzx}(\theta)$ varies linearly with θ almost up to the saturation coverage. Its phase is independent of θ.

(iii) $\Delta\chi^{(2)}_{yzy}(\theta)$ varies linearly with the coverage up to $\theta\sim 0.6$ at which a (3×1) superstructure appears. For $\theta > 0.6$, $\Delta\chi^{(2)}_{yzy}(\theta)$ remains a constant. Its phase is independent of θ for all θ.

(iv) $\Delta\chi^{(2)}_{zzz}(\theta)$ is at least one order-of-magnitude larger than $\Delta\chi^{(2)}_{xzx}(\theta)$ and $\Delta\chi^{(2)}_{zxx}(\theta)$.

V. DISCUSSION

We first note that the nonlinear-optical-interference technique can indeed be used effectively to eliminate the contribution from the adsorption-free part of the surface nonlinear response in a surface SHG measurement and allow direct measurements of the adsorption-related part versus the coverage of adsorbates. We also note that different susceptibility elements can vary with θ very differently. With the p-in, p-out geometry commonly used in surface SHG, the measured *effective surface susceptibility* is a linear combination of several susceptibility elements. Consequently, its variation with θ is further complicated by interferences between different terms. By combining the optical interference technique with different input-output polarization combinations in the SHG measurements, however, it is possible to deduce the magnitudes and the phases of various surface susceptibility elements as functions of the coverage.

Before discussing our experimental results, we first consider generally how adsorbates can affect the surface nonlinear susceptibilities. Surface nonlinearities in our case come from electronic response within the first few atomic layers at the surface of a metal. Adsorbates can influence the response of a substrate surface in a number of ways: (i) shifting the Fermi level; (ii) modifying wave functions and matrix elements; (iii) changing the density of states including the introduction of new surface states. The first mechanism is generally not significant for metals. This is due to the fact that the amount of charge transfer between adsorbates and the substrate is small compared to the number of valence electrons in a metal sample. The resulting Fermi-level shift is expected to be negligible. For the same reason, the wave functions of the band electronic states are also hardly affected. We then focus on the change of those electronic states more localized to the surface. If the adsorbate-adsorbate interaction can be neglected, then the change of surface properties including the optical response should be linear with the coverage of adsorbates. If the adsorbate-adsorbate interaction, either direct or mediated through the substrate, is not negligible and causes changes in the density of surface states or the surface resonances, we should expect the optical response to vary nonlinearly with the adsorbate coverage. The latter case is what we have observed for several nonlinear susceptibility elements of CO Ni(110).

At high CO coverages, $\theta \geq 0.6$, the LEED patterns revealed rich overlayer structures of CO as we described in Sec. IV A. They apparently result from the CO-CO interaction. Accordingly, $\Delta\chi^{(2)}_{ijk}(\theta)$ is expected to vary nonlinearly with θ. We discuss here in more detail the variation of $\Delta\chi^{(2)}_{ijk}(\theta)$ for $\theta < 0.6$. In the results presented in Sec. IV, it is interesting to note that, for $0 < \theta < 0.6$, $\Delta\chi^{(2)}_{zxx}(\theta)$ and $\Delta\chi^{(2)}_{zyy}(\theta)$ vary nonlinearly with θ, but $\Delta\chi^{(2)}_{xzx}(\theta)$ and $\Delta\chi^{(2)}_{yzy}(\theta)$ are linear with θ. Previous electron-energy-loss and low-energy electron-diffraction studies have shown that CO molecules adsorb on on-top and short-bridge sites along $[1\bar{1}0]$ with almost equal probabilities. In addition, according to Madden, Küppers, and Ertl,[18] and Bauhofer, Hock, and Küppers,[21] the binding energies of CO on the two sites are almost equal as expected and are nearly independent of the coverage. The work-function change is nearly linear with θ. These facts suggest a nearly constant charge transfer per adsorbed CO in this coverage range. Thus the nonlinear variations of $\Delta\chi^{(2)}_{zxx}(\theta)$ and $\chi^{(2)}_{zyy}(\theta)$ (in both amplitude and phase) with θ must come from the CO-CO interaction which modifies or creates new surface states. On the other hand, the linear variations of $\Delta\chi^{(2)}_{xzx}(\theta)$ and $\Delta\chi^{(2)}_{yzy}(\theta)$ with θ suggest that these two susceptibility elements do not depend significantly on the change of surface states or the resonant transitions involving such surface states. The difference between the two cases is in whether the fundamental or the second-harmonic field has a $\hat{\mathbf{z}}$ component. The $\hat{\mathbf{z}}$ component of the second harmonic is presumably able to excite surface resonant transitions but that of the fundamental cannot.

We use a simple model to give a qualitative explanation of the results. We assume that the surface nonlinear optical response comes from two separate sources: the nearly free electrons and the more localized bond electrons (strictly speaking, a clear separation of valence electrons into free and bond electrons is not possible). The adsorption of CO reduces the density of the nearly free electrons and induces new bond electronic states. We shall argue that $\Delta\chi^{(2)}_{zxx}(\theta)$ and $\Delta\chi^{(2)}_{zyy}(\theta)$ are dominated by the response of the bond electrons at the surface while $\Delta\chi^{(2)}_{xzx}(\theta)$ and $\Delta\chi^{(2)}_{yzy}(\theta)$ are dominated by the response of the nearly free electrons.

It is known that the surface SH response from a nearly-free-electron gas is very weak if the fundamental input is polarized along the surface plane.[4] Therefore, $\Delta\chi^{(2)}_{zxx}(\theta)$ and $\Delta\chi^{(2)}_{zyy}(\theta)$ obtained in the s-in, p-out geometry are likely to have contributions mainly from the bond electrons. The nonlinear variations of $\Delta\chi^{(2)}_{zxx}(\theta)$ and $\Delta\chi^{(2)}_{zyy}(\theta)$ with θ suggest that they are resonantly enhanced by transitions involving surface states affected by CO coverage. The resonance can be with either $\hbar\omega$ at $\sim$2.3 eV or $2\hbar\omega$ at $\sim$4.7 eV. That the same behavior is not observed for $\Delta\chi^{(2)}_{xzx}(\theta)$ and $\Delta\chi^{(2)}_{yzy}(\theta)$ indicates that the resonance is with $2\hbar\omega$. To support this argument, we have performed a SHG measurement with the input at 1.064 μm (i.e., $\hbar\omega = 1.67$ eV) in the p-in, p-out geometry. The effective susceptibility $\Delta\chi^{(2)}_{\text{eff}}(\theta)$, obtained by the interference technique, varies almost linearly with θ, in contrast to the case with the input at 2.33 eV reported in Fig. 2(a). Thus surface resonances involving adsorbates seem to be only important for the latter case and therefore must be with $2\hbar\omega \sim 4.7$ eV. At the *saturation coverage,* surface resonances have been identified by Kuhlenbeck *et al.*[20] and by Memmel *et al.*[19] For $\chi^{(2)}_{zxx}(\theta)$, three transitions may contribute: $d_{zz}^{+} \rightarrow 2\pi_y^{-}$(5.5 eV); $d_{xz}^{-} \rightarrow 2\pi_x^{-}$(5.5 eV); $d_{xy}^{+} \rightarrow 2\pi_x^{-}$(5.0 eV). For $\chi^{(2)}_{zyy}(\theta)$, the possibly involved transitions are the following: $d_{zz}^{+} \rightarrow 2\pi_y^{-}$(5.5 eV); $d_{xz}^{+} \rightarrow 2\pi_x^{+}$(5.5 eV); $d_{xy}^{-} \rightarrow 2\pi_x^{+}$(5.0 eV). Unfortunately, no information is available on how these surface resonances evolve with the increase of CO coverage.

The nearly free electrons *can* yield strong surface s-polarized SH response if the fundamental field has components both perpendicular and parallel to the surface.[4]

The bond electrons, on the other hand, may contribute little to the s-polarized SH response assuming that an s-polarized field cannot excite the surface resonances. We then have $\Delta\chi^{(2)}_{xzx}(\theta)$ and $\Delta\chi^{(2)}_{yzy}(\theta)$ dominated by the nearly-free-electron contribution; hence they vary linearly with θ. The interpretation here is consistent with the results of photoemission studies by Kuhlenbeck *et al.*[20] They found that the density of states of partially occupied s band and d band right below the Fermi level decreases almost linearly as θ increase from 0 to 0.6, before it ceases to change for $\theta > 0.6$.

This simple model may also explain why the nearly-free-electron model seems to be able to explain qualitatively the results of SHG from many metal surfaces with the p-in, p-out geometry.[8–12] If $\Delta\chi^{(2)}_{xzx}(\theta)$ dominates in the response because of the large Fresnel coefficient as well as the lack of surface resonant enhancement, then the nearly free electrons (assuming a division of bond electrons and nearly free electrons is permitted) are responsible for the nonlinear response and hence $\Delta\chi^{(2)}_{\text{eff}}(\theta)$ varies almost linearly with θ.[8–12] We must, however, keep in mind that the observed linear coverage dependence of $\Delta\chi^{(2)}_{ijk}(\theta)$ can just as well be accidental, due to negligible effect of the CO-CO interaction on the surface states that contribute to SHG in the specific case. Measurements with a tunable input laser beam can help to determine the importance of surface resonances.

As a final remark, we note that recently, Hamilton, Anderson, and Williams also studied the optical SHG from a CO-covered Ni(110) using 1.064 and 0.700 μm as the pump beam.[12] Although they did not perform the interference measurement, their results are consistent with ours using a pump beam at 1.064 μm, and can be interpreted as having a predominant contribution from the nearly free electrons.

VI. CONCLUSION

We have demonstrated that the coverage dependence of a surface nonlinear susceptibility can be obtained directly by using a nonlinear-optical-interference technique in SHG measurements. The technique was applied to study SHG from CO/Ni(110). The nonlinear susceptibility elements $\Delta\chi^{(2)}_{zxx}(\theta)$ and $\Delta\chi^{(2)}_{zyy}(\theta)$ vary nonlinearly with the CO coverage θ, but $\Delta\chi^{(2)}_{xzx}(\theta)$ and $\Delta\chi^{(2)}_{yzy}(\theta)$ vary linearly with θ until $\theta \sim 0.6$ where CO begins to form a (3×1) superstructure. A crude picture suggests that the former are dominated by contributions from localized electrons with surface resonance enhancement around 4.7 eV, while the latter are dominated by contributions from nearly free electrons. The CO-CO interaction affecting the surface states and modifying the surface resonances leads to the nonlinear dependence of $\Delta\chi^{(2)}_{zxx}(\theta)$ and $\Delta\chi^{(2)}_{zyy}(\theta)$ on θ. The localization of nearly free electrons by CO adsorption results in the linear decrease of $\Delta\chi^{(2)}_{xzx}(\theta)$ and $\Delta\chi^{(2)}_{yzy}(\theta)$ with θ.

ACKNOWLEDGMENTS

One of the authors (W.D.) gratefully acknowledges support by the Alexander von Humboldt Foundation, Federal Republic of Germany. One of us (R.C.) acknowledges partial support by the Natural Sciences and Engineering Research Council of Canada. This work was supported by the Director, Office of Energy Research, Office of Basic Energy Sciences, Materials Sciences Division of the U.S. Department of Energy under Contract No. DE-AC-3-76SF00098.

*Permanent address: Institut für Grenzflächenforschung and Vakuumphysik, Kernforschungsanlage, D-5170 Jülich, Germany.

[1]Y. R. Shen, Annu. Rev. Phys. Chem. **40**, 327 (1989), and extensive references therein.

[2]X. D. Zhu, Th. Rasing, and Y. R. Shen, Phys. Rev. Lett. **61**, 2883 (1988).

[3]R. Murphy, M. Yeganeh, K. J. Song, and E. W. Plummer, Phys. Rev. Lett. **63**, 318 (1989).

[4]A. Liebsch, Phys. Rev. Lett. **61**, 1233 (1988); A. Liebsch and W. L. Schaich, Phys. Rev. B **40**, 5401 (1989); J. Rudnick and G. I. Stern, *ibid.* **4**, 4272 (1971).

[5]P. Guyot-Sionnest, A. Tadjeddine, and A. Liebsch, Phys. Rev. Lett. **64**, 1678 (1990); G. L. Richmond, J. M. Robinson, and V. L. Shannon, Prog. Surf. Sci. **28**, 1 (1989).

[6]X. D. Zhu, Th. Rasing, and Y. R. Shen, Chem. Phys. Lett. **155**, 459 (1989).

[7]P. Guyot-Sionnest and Y. R. Shen, Phys. Rev. B **38**, 7985 (1988).

[8]H. W. K. Tom, C. M. Mate, X. D. Zhu, J. E. Crowell, T. F. Heinz, G. A. Somorjai, and Y. R. Shen, Phys. Rev. Lett. **52**, 348 (1984).

[9]X. D. Zhu, Y. R. Shen, and R. Carr, Surf. Sci. **163**, 114 (1985).

[10]S. G. Grubb, A. M. DeSantolo, and R. B. Hall, J. Phys. Chem. **92**, 1419 (1988).

[11]J. C. Hamilton and R. J. M. Anderson, Chem. Phys. Lett. **151**, 455 (1988).

[12]J. C. Hamilton, R. J. M. Anderson, and L. R. Williams, J. Vac. Sci. Technol. B **7**, 1208 (1989).

[13]J. J. Wynne and N. Bloembergen, Phys. Rev. **188**, 1211 (1969), and references therein.

[14]K. Kemnitz, K. Bhattacharyya, J. M. Hicks, G. R. Pinto, K. B. Eisenthal, and T. F. Heinz, Chem. Phys. Lett. **131**, 285 (1986).

[15]Y. R. Shen, *The Principles of Nonlinear Optics* (Wiley, New York, 1984), p. 27.

[16]R. J. Behm, G. Ertl, and V. Penka, Surf. Sci. **160**, 387 (1985).

[17]T. N. Taylor and P. J. Estrup, J. Vac. Sci. Technol. **10**, 26 (1973).

[18]H. H. Madden, J. Küppers, and G. Ertl, J. Chem. Phys. **58**, 3401 (1973).

[19]N. Memmel, G. Rangelov, E. Bertel, V. Dose, K. Kometer, and N. Rösch, Phys. Rev. Lett. **63**, 1884 (1989).

[20]H. Kuhlenbeck, H. B. Saalfeld, U. Buskotte, M. Neumann, H. J. Freud, and E. W. Plummer, Phys. Rev. B **39**, 3475 (1989).

[21]M. Nishijima, S. Masuda, Y. Sakisaka, and M. Onchi, Surf. Sci. **107**, 31 (1981); J. Bauhofer, M. Hock, and J. Küppers, *ibid.* **191**, 395 (1987); J. C. Bertolini and B. Tardy, *ibid.* **102**,

131 (1981); B. J. Bandy, M. A. Chesters, P. Hollins, J. Pritchard, and N. Sheppard, J. Mol. Struct. **80**, 203 (1982).

[22]B. Voigtländer, D. Brunchmann, S. Lehwald, and H. Ibach, Surf. Sci. **225**, 151 (1990).

[23]W. Riedl and D. Menzel, Surf. Sci. **163**, 39 (1985); M. D. Alvey, M. J. Dresser, and J. T. Yates, Jr., *ibid.* **165**, 447 (1986); D. A. Wesner, F. P. Coenen, and H. P. Bonzel, *ibid.* **199**, L419 (1988); D. J. Hannman and M. A. Passler, *ibid.* **203**, 449 (1988).

[24]J. Küppers, Surf. Sci. **36**, 53 (1973).

[25]S. Lehwald (private communication).

[26]C. M. Mate, G. A. Somorjai, H. W. K. Tom, X. D. Zhu, and Y. R. Shen, J. Chem. Phys. **88**, 441 (1988).

[27]L. E. Urbach, J. M. Hicks, K. L. Percival, E. W. Plummer, and H.-L. Dai (private communication).

[28]J. H. Weaver, C. Krafka, D. W. Lynch, and E. E. Koch, *Optical Properties of Metals* (Fach-Informations-Zentrum Energie, Physik, Mathematick GmbH, Karlsruhe, 1981), pp. 96–108.